

# Using Differential Phases in Optical Interferometry

Henrique R. Schmitt<sup>a,b</sup>, Thomas A. Pauls<sup>a</sup>, Christopher Tycner<sup>c</sup>, J. Thomas Armstrong<sup>a</sup>, James, A. Benson<sup>c</sup>, James H. Clark<sup>a</sup>, Robert B. Hindsley<sup>a</sup>, Donald, J. Hutter<sup>c</sup>, Deane M. Peterson<sup>d</sup>, Anders M. Jorgensen<sup>e</sup>, David Mozurkewich<sup>f</sup>, G. Charmaine Gilbreath<sup>g</sup>, Robert T. Zavala<sup>c</sup>

<sup>a</sup> Naval Research Laboratory, Code 7215, 4555 Overlook Avenue SW, Washington, DC 20375, USA;

<sup>b</sup> Interferometrics, Inc., Herndon, VA 20171, USA;

<sup>c</sup> US Naval Observatory, Flagstaff Station, 10391 West Naval Observatory Road, Flagstaff, AZ 86001-8521, USA;

<sup>d</sup> Department of Physics and Astronomy, Stony Brook University, Stony Brook, NY 11794, USA;

<sup>e</sup> Los Alamos National Laboratory, ISR-4, D448, P.O. Box 1663, Los Alamos, NM 87545, USA

<sup>f</sup> Seabrook Engineering, 9310 Dubarry Ave., Seabrook, MD 20706, USA

<sup>g</sup> Naval Research Laboratory, Code 5505, 4555 Overlook Avenue SW, Washington, DC 20375, USA;

## ABSTRACT

We present the results of differential phase experiments done with data from the Navy Prototype Optical Interferometer (NPOI). We take advantage of the fact that this instrument simultaneously records 16 spectral channels in the wavelength range 550-850nm, for multiple baselines. We discuss the corrections applied to the data, and show the results obtained for Vega and the Be star  $\beta$  Lyrae.

**Keywords:** optical interferometry, NPOI, differential phases, stars, circumstellar disks

## 1. INTRODUCTION

Differential phase is a powerful technique used to measure small phase variations as a function of wavelength, due to sources with chromatic, asymmetric structures. Previous applications of differential phase include the study of H $\alpha$  disks and envelopes around stars,<sup>12,13</sup> and the detection of phase fluctuations due to a binary companion.<sup>1</sup> Since this technique relies on simultaneous multiwavelength phase measurements, it is ideally suited for NPOI observations. In the following we describe the first tests of this technique on NPOI data from a star with a circumnuclear H $\alpha$  disk and from an asymmetric star.

## 2. OBSERVATIONS AND DETERMINATION OF DIFFERENTIAL PHASES

The observations presented in this paper were obtained with the NPOI<sup>2</sup> on the nights of 2004-09-01 and 2005-05-19. These observations were done with 2 spectrographs, simultaneously recording 16 channels in the wavelength range 550-850nm, and 3 baselines per spectrograph. The first set of observations used baselines with lengths between 18 m and 64 m, while in the second run the longest baseline was of the order of  $\sim$ 53 m. The night of 2004-09-01 was used to observe several scans of Vega ( $\alpha$  Lyrae), its calibrators ( $\gamma$  Lyrae) and other stars, while on 2005-05-19 we obtained 9 scans of  $\beta$  Lyrae and its calibrator  $\gamma$  Lyrae. Each scan had a duration of 30 s, and the observations of the program star were interleaved with observation of its calibrator.

The data reduction started with the coherent integration of complex visibilities, which was done applying the algorithm developed by Ref. 5 (see Refs. 6, 7 for a new coherent integration algorithm). This technique uses

---

Further author information: (Send correspondence to Henrique R. Schmitt)  
H.R.S.: E-mail: henrique.schmitt@nrl.navy.mil

# Report Documentation Page

Form Approved  
OMB No. 0704-0188

Public reporting burden for the collection of information is estimated to average 1 hour per response, including the time for reviewing instructions, searching existing data sources, gathering and maintaining the data needed, and completing and reviewing the collection of information. Send comments regarding this burden estimate or any other aspect of this collection of information, including suggestions for reducing this burden, to Washington Headquarters Services, Directorate for Information Operations and Reports, 1215 Jefferson Davis Highway, Suite 1204, Arlington VA 22202-4302. Respondents should be aware that notwithstanding any other provision of law, no person shall be subject to a penalty for failing to comply with a collection of information if it does not display a currently valid OMB control number.

1. REPORT DATE <b>2006</b>		2. REPORT TYPE		3. DATES COVERED <b>00-00-2006 to 00-00-2006</b>	
4. TITLE AND SUBTITLE <b>Using Differential Phases in Optical Interferometry</b>				5a. CONTRACT NUMBER	
				5b. GRANT NUMBER	
				5c. PROGRAM ELEMENT NUMBER	
6. AUTHOR(S)				5d. PROJECT NUMBER	
				5e. TASK NUMBER	
				5f. WORK UNIT NUMBER	
7. PERFORMING ORGANIZATION NAME(S) AND ADDRESS(ES) <b>Naval Research Laboratory, Code 7215, 4555 Overlook Avenue SW, Washington, DC, 20375</b>				8. PERFORMING ORGANIZATION REPORT NUMBER	
9. SPONSORING/MONITORING AGENCY NAME(S) AND ADDRESS(ES)				10. SPONSOR/MONITOR'S ACRONYM(S)	
				11. SPONSOR/MONITOR'S REPORT NUMBER(S)	
12. DISTRIBUTION/AVAILABILITY STATEMENT <b>Approved for public release; distribution unlimited</b>					
13. SUPPLEMENTARY NOTES					
14. ABSTRACT <b>We present the results of differential phase experiments done with data from the Navy Prototype Optical Interferometer (NPOI). We take advantage of the fact that this instrument simultaneously records 16 spectral channels in the wavelength range 550-850nm, for multiple baselines. We discuss the corrections applied to the data, and show the results obtained for Vega and the Be star &amp;#946; Lyrae.</b>					
15. SUBJECT TERMS					
16. SECURITY CLASSIFICATION OF:			17. LIMITATION OF ABSTRACT <b>Same as Report (SAR)</b>	18. NUMBER OF PAGES <b>8</b>	19a. NAME OF RESPONSIBLE PERSON
a. REPORT <b>unclassified</b>	b. ABSTRACT <b>unclassified</b>	c. THIS PAGE <b>unclassified</b>			

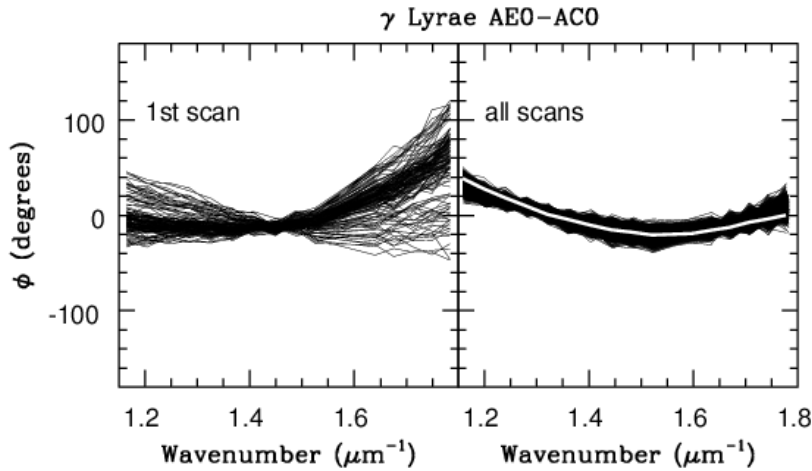


**Figure 1.** This figure presents baseline phases (AEO-ACO, 18 m) of  $\gamma$  Lyrae as a function of wavenumber. The left panel shows the raw phases from the first scan observed in the night of 2005-05-19. Each individual line corresponds to a coherently integrated subscan with a duration of 200 ms. The right panel shows, as a white line, the average of all calibrator scans obtained on this night, including  $\gamma$  Lyrae. The black lines correspond to all 200 ms coherently integrated subsamples of  $\gamma$  Lyrae observed on that night (1728 in total), corrected for differential atmospheric delays to match the white line.

the deviation of the calculated fringe position from the estimated geometrical value to rotate the phasors onto a common fringe. The aligned phasors are then averaged into 200 ms subsamples ( $100 \times 2$  ms instrumental integration times), and the phases are calculated for the individual channels.

The results of this procedure are presented in the left panel of Fig. 1, where we show the phases for each 200 ms subscan of the first scan of the calibrator star  $\gamma$  Lyrae. We can see that the individual subscan phases follow smooth curves with similar shapes. Another important result that can be seen in this figure is the fact that the subsamples with high phase values in the red have lower ones in the blue, and vice-versa. Since this star is not resolved by these observations it should have zero phase on average, so the observed phases can be attributed to uncompensated glass and differential airpath between the two beams. The effect of uncompensated glass is not expected to vary significantly over the course of the night, or even over the course of several days, so we can identify this effect as being responsible for the overall shape of the curves in the left panel. The variable component, responsible for the subscan to subscan variations can be identified with the effect due to differential airpath delay between the two stations. This effect adds a quadratic phase as a function of wavenumber to the data.

In the right panel of Fig. 1 we show that fitting and subtracting a curve of the form  $y = a + bx + cx^2$  ( $x$  is wavenumber), to the variable phase component of the subsamples, we can reduce them to a common curve, shown in white. This curve corresponds to the average of all calibrator scans observed throughout the night. By averaging all these scans we basically eliminate the differential airpath delay effects, under the reasonable assumption that the mean airpath difference over the course of a night is zero, and are left only with the instrumental phases (uncompensated glass). The black lines show all the 200 ms subsamples of  $\gamma$  Lyrae observed on that night (1728 in total), after fitting and subtracting the function described above. Notice that all lines cluster around the white line.

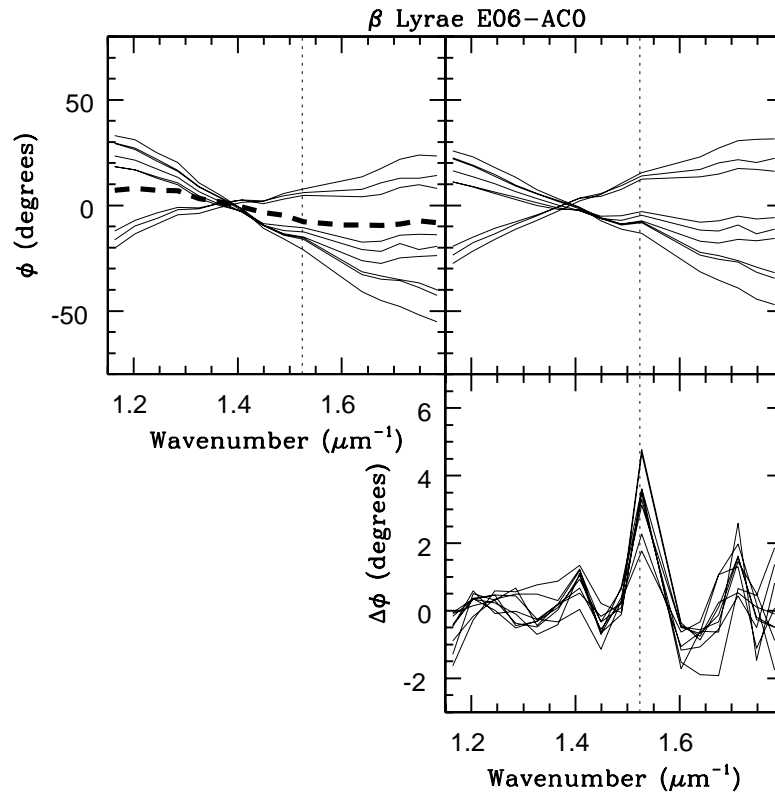


**Figure 2.** This figure shows the phases of the Be star  $\beta$  Lyrae on the long baseline E06-AC0 (34.2 m), observed on 2005-05-19. The top left panel shows the instrumental phases (dashed line) and the average phases of 9 individual scans (solid lines), as a function of wavenumber. The vertical dotted line shows the location of  $H\alpha$ . The top right panel shows the phases of each scan after the subtraction of the instrumental contribution. The bottom panel shows the residuals obtained after fitting a curve of the form  $y = a + bx + cx^2$  to the continuum points of each individual curve in the top right panel, and subtracting it from all the channels, including  $H\alpha$ . The uncertainty in the phases is of the order of  $0.5^\circ$ .

## 2.1. $\beta$ Lyrae

The results presented in Fig. 1 show that in the case of calibrator stars, which are symmetric and the phase is intrinsically zero, we can determine and correct the instrumental phases, as well as the effects due to differential airpath between two stations. We show in Fig. 2 the application of this technique to one of the baselines of the Be star  $\beta$  Lyrae, where we aim at detecting the phases of the H $\alpha$  channel. This is a binary system,<sup>4</sup> only partially resolved by our observations, where both components have similar magnitudes and colors, so the system is approximately symmetric and should have phases close to zero in the continuum channels. However, in the case of the H $\alpha$  channel we expect to see a phase signature. This line originates in a disk  $\sim 2$  mas in diameter, that surrounds only one of the stars in the system. As a result of this geometry, the H $\alpha$  photocenter is displaced relative to the photocenter of the binary system, and should show a differential phase relative to the continuum.

We followed the same reduction steps discussed above, but analyze the average of each 30 s scan, instead of the individual 200 ms subscans. We take advantage of the fact that the differential airpath effects are additive, so we can fit and subtract the effective contribution of this effect to the average scan of a source. The top left panel of Fig. 2 shows the average phases of the 9 scans of  $\beta$  Lyrae, the instrumental phase obtained from the average of all calibrator scans and also indicate the location of the H $\alpha$  line. The top right panel shows the phases obtained after the subtraction of the instrumental phases, which leaves only the phases due to the source and differential airpath. We can see that the phases, as in the case of the calibrator star  $\gamma$  Lyrae, vary smoothly with wavelength, except for a clear deviation in the H $\alpha$  channel. The correction for the effect of differential airpath is done by assuming that the phases should be zero in the continuum channels, so their phases were fitted as in the case of  $\gamma$  Lyrae, and subtracted from all channels, including H $\alpha$ . The residuals from this operation are presented in the bottom right panel of the figure, where we can see that the final continuum phases cluster around zero and the H $\alpha$  phases show a clear signal.

The differential phases of  $\beta$  Lyrae, for all baselines observed in 2005-05-19, are presented in Fig. 3. As in Fig. 2, we can see that the strongest phase signal is in H $\alpha$ , with the continuum differential phases usually clustering around zero. We also see some deviations from zero around  $1.4\mu\text{m}^{-1}$  and  $1.7\mu\text{m}^{-1}$ , which correspond to the neutral Helium lines at 706.5 nm and 587.6 nm, respectively. Other deviations from zero in the continuum channels can be due to atmosphere or instrument effects, and require further investigation. A particularly interesting result from this figure is the fact that the larger phase variations occur along the E-W baselines. This indicates that the binary and the disk are extended along this direction, consistent with the non-resolution of the binary by the GI2T interferometer,<sup>8</sup> which had a N-S orientation.

## 2.2. VEGA

Another application of the differential phases technique is the study of stellar structure. Here we present the particularly interesting case of Vega ( $\alpha$  Lyrae), the primary standard calibration star. Recent observations by NPOI<sup>10</sup> and CHARA<sup>3</sup> showed that this is a rapidly rotating star ( $\sim 93\%$  of the breakup velocity), seen almost pole-on ( $i = 4.54^\circ$  along  $p.a. = 8.6^\circ$ ). The effects of the rotation cause the star to have an equatorial radius 1.246 times larger than the polar one, and a temperature drop of  $\sim 2400$  K from the poles to the equator. These properties make the star look asymmetric when seen projected in the sky, an effect that produces a strong phase signature at wavelengths around the first null crossing (this signature was used by Ref. 10 to fit the properties of this star).

We show in the top panels of Fig. 4 and Fig. 5 the predicted differential phases of Vega for the baseline W07-AE0 (64.4 m), observed on 2004-09-01 at hour angles of 2.92 h and 3.55 h, respectively. This figure shows the first null crossing around 700 nm and 670 nm (phase flip of  $180^\circ$ ), where we can also see the large phase deviations due to the asymmetry of the star. The bottom panels of the figures show the observed differential phases, after a first order subtraction of the differential airpath. We can see that we detect, in both cases, a phase signature similar to the predicted one, but with some small differences. In the case of Fig. 4, the observed phase flip happens at a higher wavelength relative to the predicted value. Also, the amplitude of the phase flips does not match the predicted values in both cases. We attribute these differences to wavelength calibration errors and cross talk effects,<sup>11</sup> and are currently investigating other possible explanations.

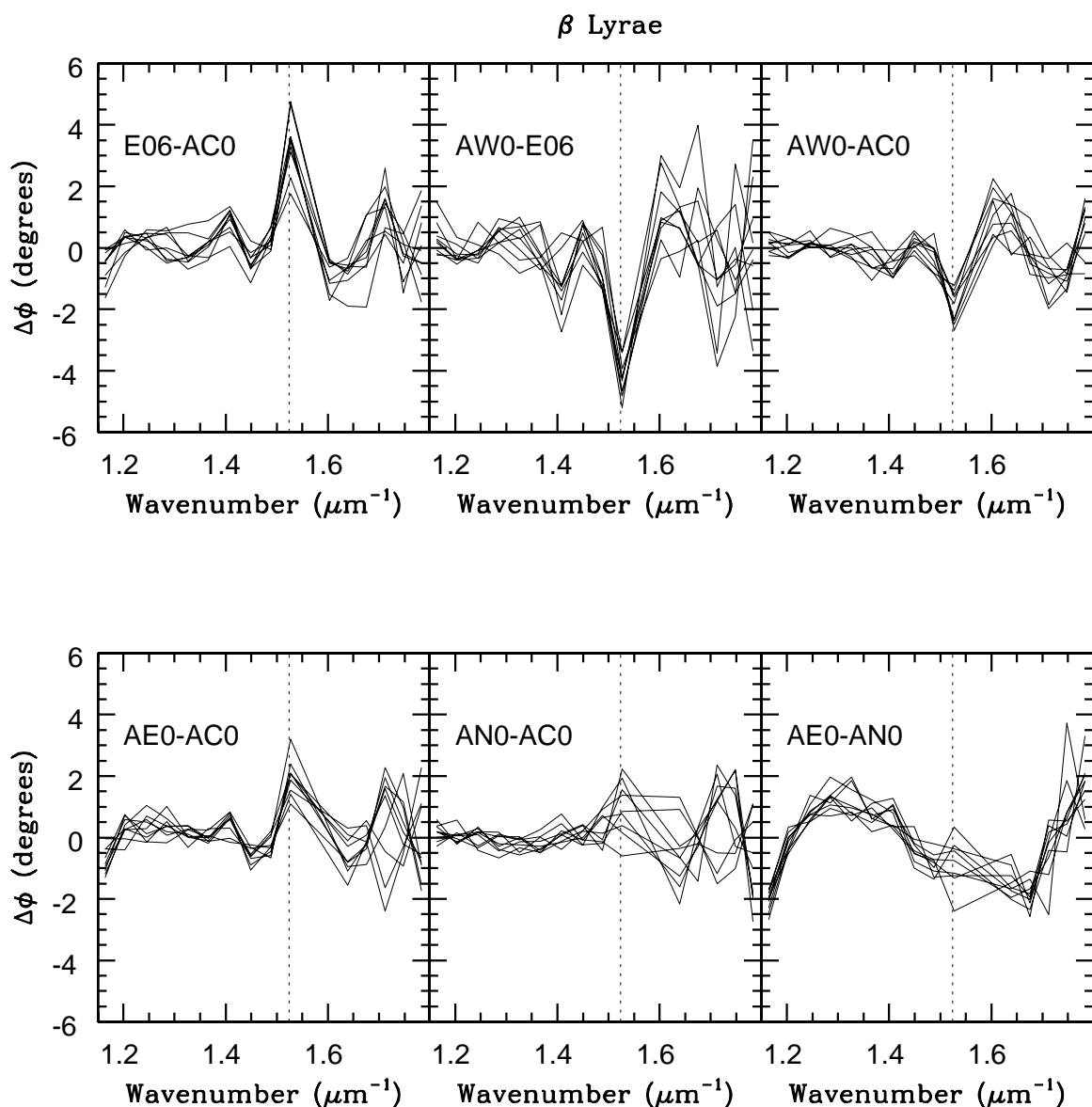


**Figure 3.** Residual phases of  $\beta$  Lyrae, calculated for 6 different baselines observed on 2005-05-19 (E06-AC0=34.2 m, AW0-E06=53.2 m, AW0-AC0=22.2 m, AE0-AC0=18.9 m, AN0-AC0=22.9 m, AE0-AN0=34.9 m) . Each row corresponds to a different spectrograph. Each solid line is a different scan and the dotted lines indicate the position of H $\alpha$ .

### 3. SUMMARY

We presented the results of differential phase experiments done with multiwavelength data from the NPOI. We discussed the reductions applied to the data, the correction of phases due to instrumental effects and differential airpath between stations. We presented the application of this technique to the Be star  $\beta$  Lyrae, which shows a strong differential phase signature in the H $\alpha$  channel, particularly along the E-W baselines, consisted with previous results. Further applications of this technique to Be stars include the determination of complex visibilities

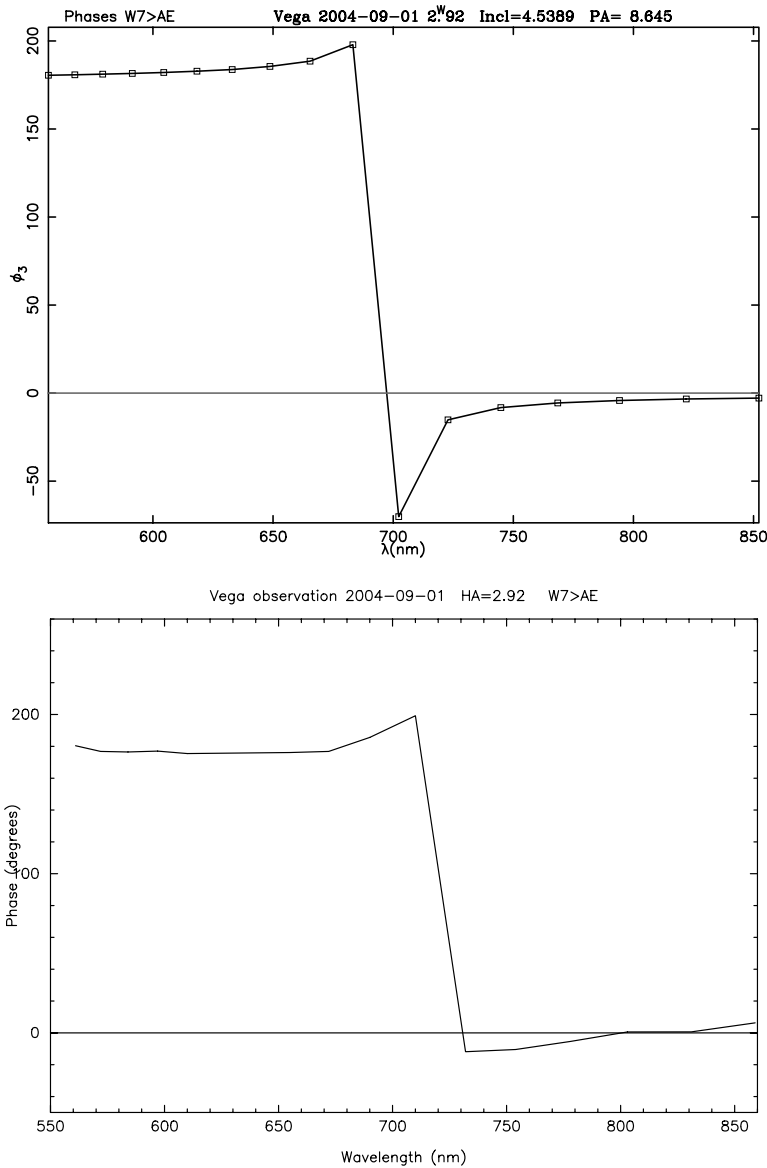


**Figure 4.** The top panel shows the predicted differential phases of Vega, based on NPOI results from Ref. 10 (inclination and position angle of the pole are indicated on the top of the panel), for observations with the baseline W7-AE (64.4 m) on the night of 2004-09-01 at an hour angle of 2.92 h. The bottom panel shows the corresponding observed differential phases, after the correction for instrumental effects and a first order subtraction of the differential airpath effects.

and the imaging of their  $H\alpha$  disks using standard radio interferometry software, presented in this conference by Ref. 9. We also presented the case of Vega, a rapidly rotating star seen almost pole-on. We show that we can see the phase signature due to the asymmetric structure of the star, but we still need to understand some instrument issues, like cross talk, in order to further improve the use of this technique to other stars. This technique will be useful for the detection of asymmetric structures, due to rotation, flares or spots, in other stars.

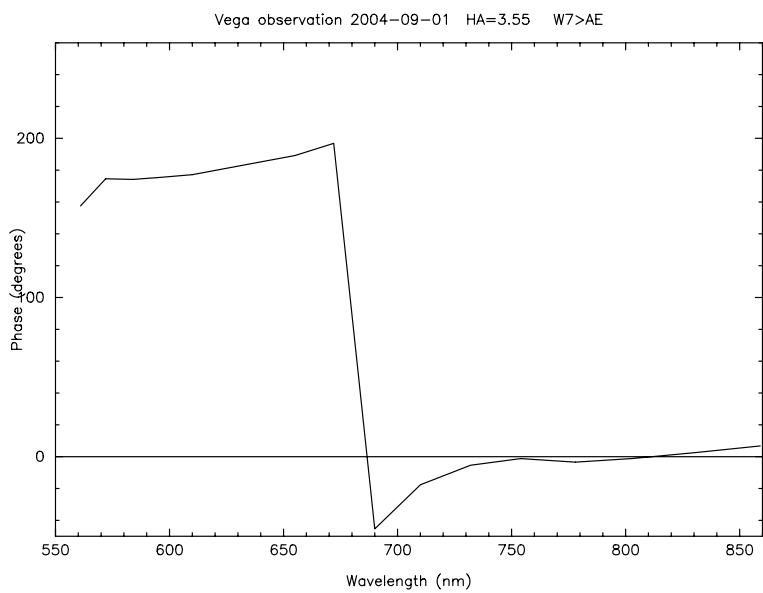
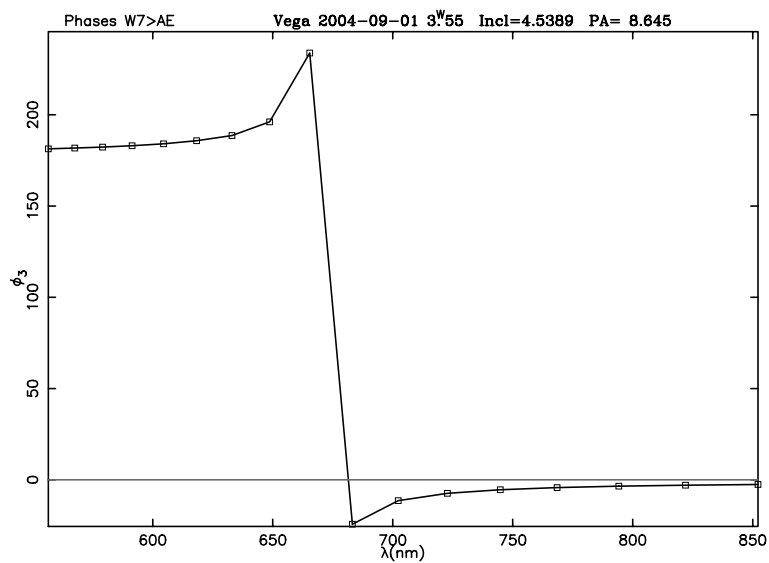


Figure 5. Same as Figure 4 for hour angle 3.55 h.

## ACKNOWLEDGMENTS

The Navy Prototype Optical Interferometer is a joint project of the Naval Research Laboratory and the US Naval Observatory, in cooperation with Lowell Observatory, and is funded by the Office of Naval Research and the Oceanographer of the Navy. C. T. acknowledges that this work was performed under a contract with the Jet Propulsion Laboratory (JPL) funded by NASA through the Michelson Fellowship Program, while being employed by NVI, Inc. at the US Naval Observatory. JPL is managed for NASA by the California Institute of Technology.

## REFERENCES

1. Akeson, R. L., Swain, M. R., & Colavita, M. M. 2000, Proc. SPIE Vol. 4006, p. 321-327, Interferometry in Optical Astronomy, Pierre J. Lena; Andreas Quirrenbach; Eds.
2. Armstrong, J. T., Mozurkewich, D., Rickard, L. J., Hutter, D. J., Benson, J. A., Bowers, P. F., Elias, N. M., Hummel, C. A., Johnston, K. J., Buscher, D. F., Clark, J. H., Ha, L., Ling, L.-C., White, N. M., Simon, R. S. 1998, ApJ, 496, 550
3. Aufdenberg, J. P., Merand, A., Coude du Foresto, V., Absil, O., Di Folco, E., Kervella, P., Ridgway, S. T., Berger, D. H., ten Brummelaar, T. A. McAlister, H. A., Sturmman, J., Sturmman, L., Turner, N. H. 2006, ApJ, in press (astro-ph/0603327)
4. Harmanec, P. 2002, AN, 323, No. 2, 87
5. Hummel, C. A., Mozurkewich, D., Benson, J. A., & Wittkowski, M. Interferometry for Optical Astronomy II. Edited by Wesley A. Traub. Proceedings of the SPIE, Volume 4838, p. 1107 (2003)
6. Jorgensen, A. M., Mozurkewich, D., Armstrong, T., Hindsley, R., Pauls, T. A., Gilbreath, C., & Restaino, S. New Frontiers in Stellar Interferometry, Edited by Wesley A. Traub, Proceedings of SPIE Volume 5491, p.1474 (2004)
7. Jorgensen, A. M., Mozurkewich, D., Schmitt, H., Armstrong, T., Gilbreath, C., Hindsley, R., Pauls, T. A., Peterson, D. Advances in Stellar Interferometry, Proceedings of the SPIE, Volume 6268
8. Mourard, D., Bonneau, D., Biazit, A., Labeyrie, A., Morand, F., Percheron, I., Tallon-Bosc, I., Vakili, F. 1992, in: H. A. McAlister, W. I. Hartkopf (eds.), *Complementary approaches to double and multiple star research*, ASP Conf. Ser. Vol 32, p. 510
9. Pauls, T. A., Schmitt, H. R., Tycner, C., Armstrong, J. T., Benson, J., Clark, J., Gilbreath, G. C., Hindsley, R. B., Hutter, D., & Jorgensen, A. M. Advances in Stellar Interferometry, Proceedings of the SPIE, Volume 6268
10. Peterson, D. M., Hummel, C. A., Pauls, T. A., Armstrong, J. T., Benson, J. A., Gilbreath, G. C., Hindsley, R. B., Hutter, D. J., Johnston, K. J., Mozurkewich, D., & Schmitt, H. R. 2006, Nature, 440, 896
11. Schmitt, H. R., Armstrong, J. T., Hindsley, R. B., & Pauls, T. A. 2005, AAS, 206, 15.01
12. Vakili, F., Mourard, D., Bonneau, D., Morand, F., & Stee, P. 1997, A&A, 323, 183
13. Vakili, F., Mourard, D., Stee, P., Bonneau, D., Berio, P., Chesneau, O., Thureau, N., Morand, F., Labeyrie, A., & Tallon-Bosc, I. 1998, A&A, 335, 261